

Enhanced Electrocatalytic Activity of low-cost NiO Microflowers on Graphene Paper for Oxygen Evolution Reaction

Luca Bruno^{1,2}, Mario Scuderi³, Francesco Priolo¹, Salvo Mirabella^{1,2}*

¹ Dipartimento di Fisica e Astronomia “Ettore Majorana”, Università degli Studi di Catania,
via S. Sofia 64, 95123, Catania, Italy

² IMM-CNR (Catania Università), via S. Sofia 64, 95123, Catania, Italy.

³ IMM-CNR, VIII strada 5, 95121 Catania, Italy.

ELECTRONIC SUPPLEMENTARY INFORMATION

Corresponding Author

*salvo.mirabella@dfa.unict.it

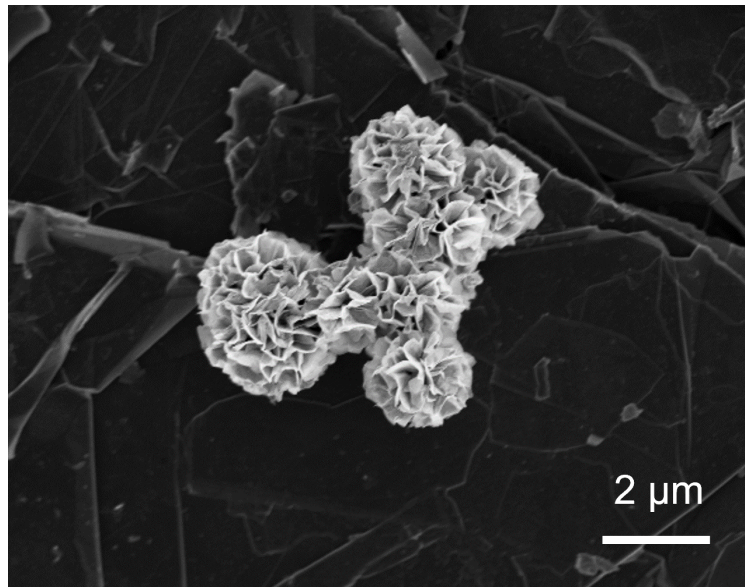


Figure S1: SEM images of NiO μ Fs on GP after electrochemical tests.

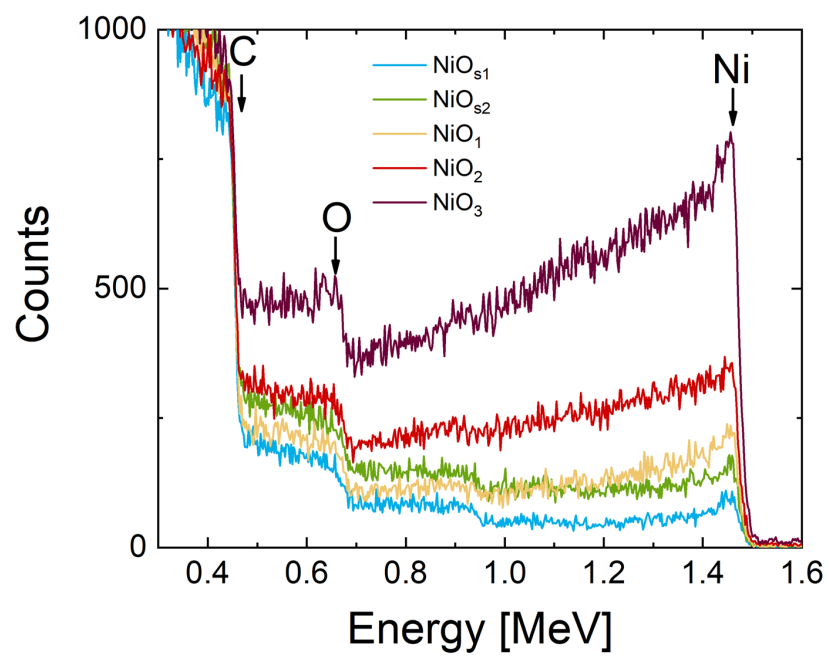


Figure S2: RBS spectra of NiO μ Fs on GP.

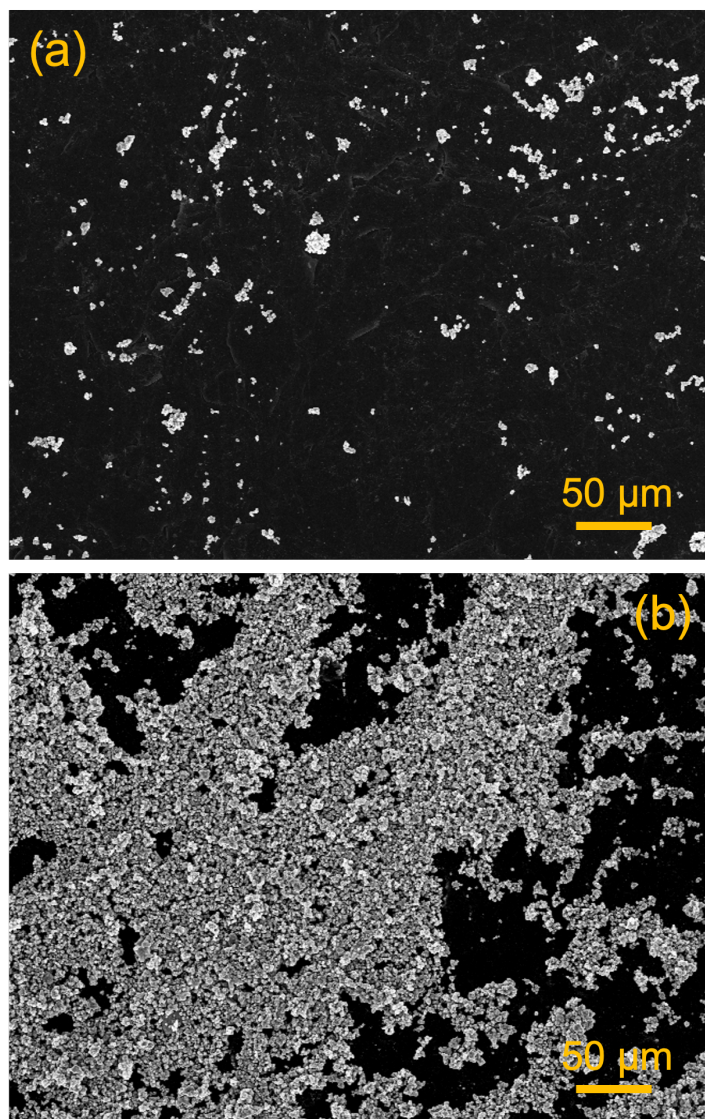


Figure S3: SEM images of NiO μ Fs on GP deposited via (a) spin coating or (b) drop casting.

Sample	R_u [Ω]	R_{ct} [Ω]	R_p [Ω]	C_{dl} [$mF s^{n-1}$]	n_1	C_p [$mF s^{n-1}$]	n_2
NiO _{s1}	4.67 ± 0.01	2.71 ± 0.03	18.6 ± 0.1	6.05 ± 0.08	0.8	2.38 ± 0.04	0.6
NiO _{s2}	4.44 ± 0.03	2.00 ± 0.06	12.9 ± 0.2	6.93 ± 0.2	0.8	2.35 ± 0.2	0.6
NiO _{D1}	5.47 ± 0.02	0.68 ± 0.02	13.1 ± 0.1	6.89 ± 0.08	0.8	1.84 ± 0.05	0.8
NiO _{D2}	4.78 ± 0.01	0.61 ± 0.03	11.1 ± 0.1	7.3 ± 0.1	0.8	1.3 ± 0.5	0.7
NiO _{D3}	4.54 ± 0.01	0.43 ± 0.02	10.3 ± 0.1	9.87 ± 0.08	0.9	0.62 ± 0.06	0.6

Table S1: EIS fitting parameters.

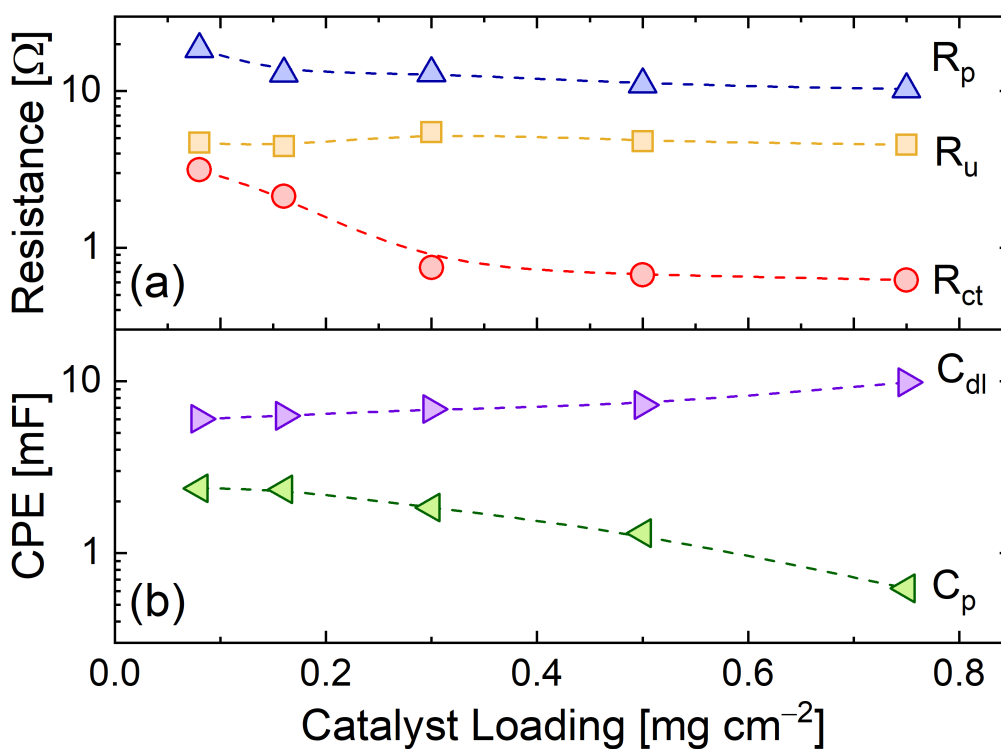
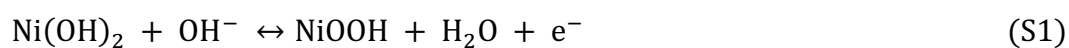


Figure S4: Behavior of equivalent circuit elements as a function of mass loading.

OER MECHANISM AT NICKEL-BASED ELECTRODES.

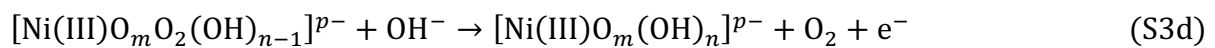
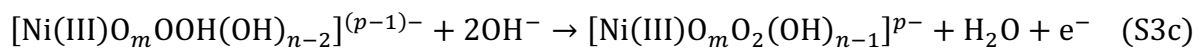
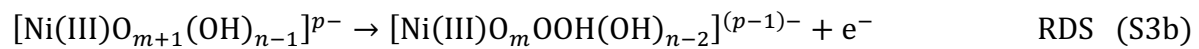
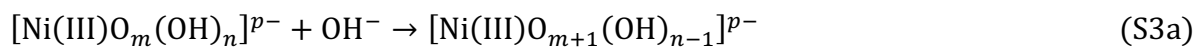
Nickel-based materials are considered some of the most promising transition metal catalysts for the Oxygen Evolution Reaction (OER) in alkaline media^{1,2}. Subsequently to the immersion of NiO electrodes in an aqueous solution a layer of Ni(OH)₂ is spontaneously formed at open circuit potential². During the oxidation/reduction cycling the Ni hydroxide layer grows after the conversion of Ni(II) to Ni(III) and the formation of NiOOH during the charge step and the re-formation of Ni(OH)₂ during the discharge step of the cyclic voltammetry³. The charge/discharge process of the NiO/ Ni(OH)₂ electrode can be described as follows⁴:



Upon the growth of the Ni(OH)₂ layer, a significant increase in the OER activity is generally observed for a hydrous nickel oxide electrodes⁵. Besides the formation of a stable and optimal

Ni(OH)₂ layer and the formation of different charge/discharge phases⁶ after potential cycling, an increase of roughness and of the number of electrochemically active sites on surface is observed¹.

In terms of a mechanistic analysis of the OER, the major difficulty is represented by the fact that the OER is a complex process involving the transfer of four electrons. Since electrons are transferred one by one, the process will be multistep⁷. Among different proposed mechanisms present in literature, Lyons *et al.*^{2,7,8} suggested a mechanistic pathway which involves intermediate species in the Ni(III) valence state. For the case of anodic oxide covered Ni anodes such a pathway might be written as follows⁹:



According to this mechanism the rate determining step (RDS) for the OER is represented by the formation of a superoxy-(OOH) species by the addition of an OH⁻ ion on top of an adsorbed oxygen atom with a Tafel slope of around 40 mV dec⁻¹.

MASS ACTIVITY DETERMINATION.

Mass activity is defined as the ratio between a fixed current density j and the catalyst loading. In our case we calculate the mass activity at a current density of 10 mA cm⁻² by using the following expression:

$$\text{Mass activity} = \frac{j [\text{A cm}^{-2}]}{\text{catalyst loading} [\text{mg cm}^{-2}]} \quad (\text{S4})$$

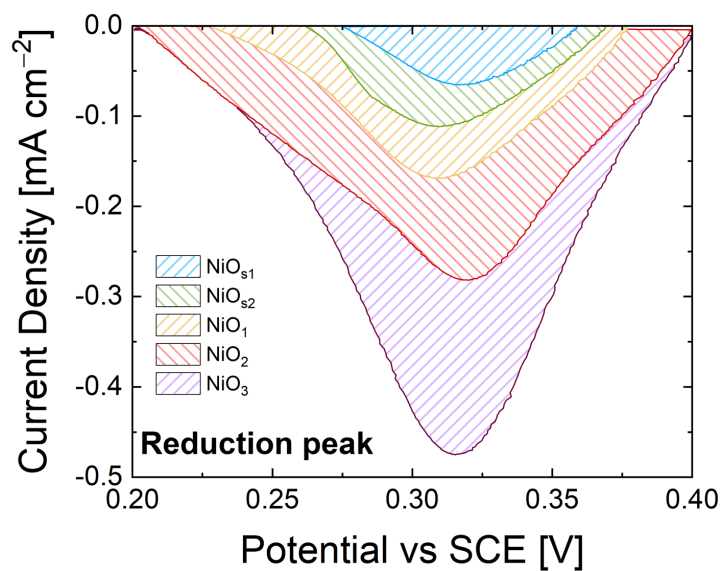


Figure S5: Reduction peaks of NiO electrodes after the first backward scan during CV.

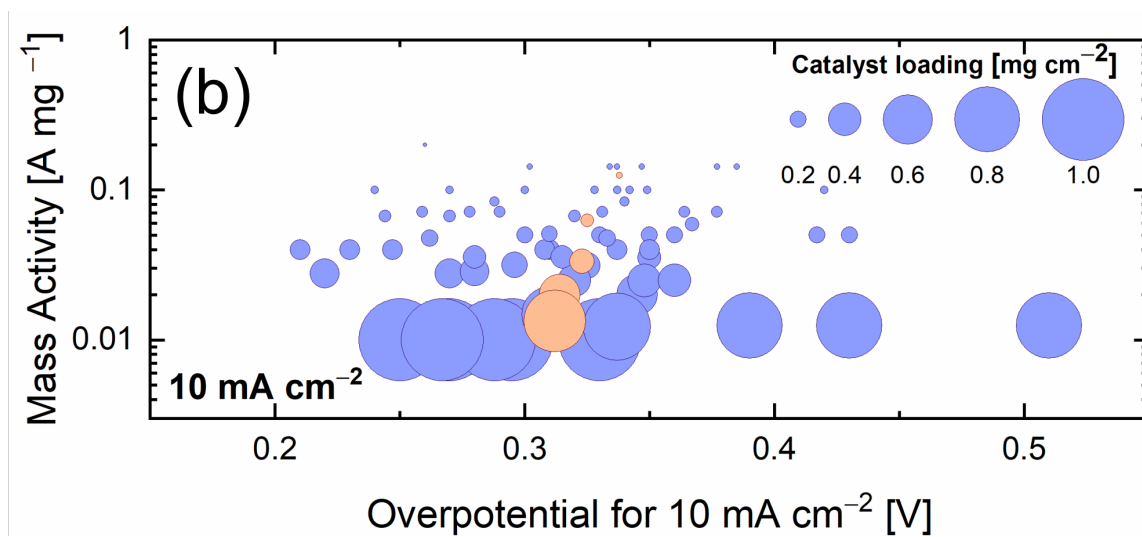


Figure S6: Mass activity at 10 mA cm^{-2} as a function of the overpotential and the catalyst loading [adapted from 10].

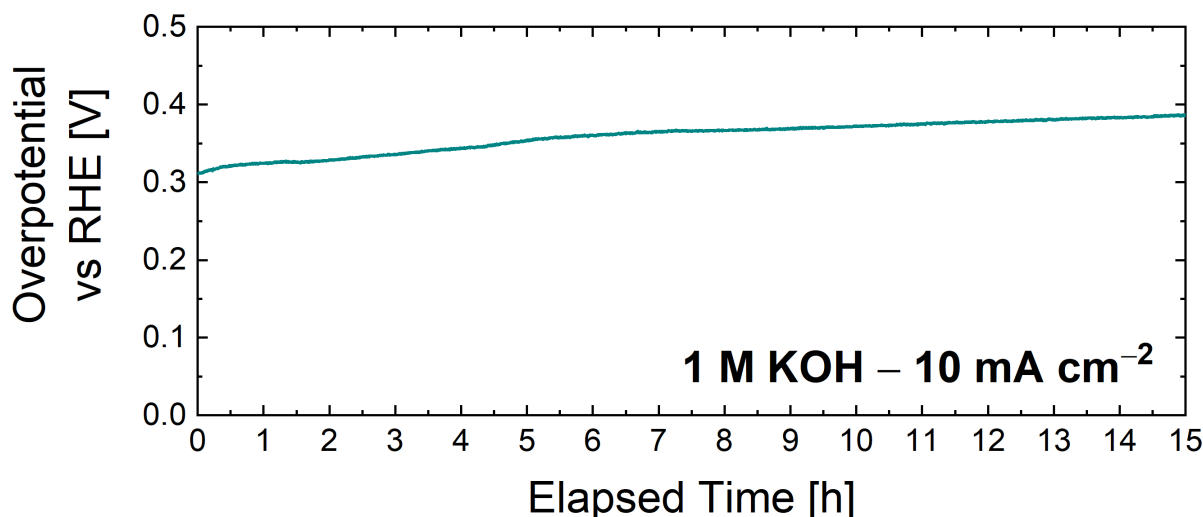


Figure S7: Chronopotentiometric test of NiO_{D2} electrode.

REFERENCES

1. E. Fabbri, A. Habereder, K. Waltar, R. Kötz and T. J. Schmidt, *Catal. Sci. Technol.*, 2014, DOI:10.1039/c4cy00669k.
2. M. E. G. Lyons and M. P. Brandon, *Int. J. Electrochem. Sci.*, 2008, 3, 1425-1462.
3. D. S. Hall, D. J. Lockwood, C. Bock and B. R. MacDougall, *Proc. R. Soc. A Math. Phys. Eng. Sci.*, 2015, DOI:10.1098/rspa.2014.0792.
4. S. Cosentino, M. Urso, G. Torrisi, S. Battiato, F. Priolo, A. Terrasi and S. Mirabella, *Mater. Adv.*, 2020, DOI:10.1039/d0ma00467g.
5. I. J. Godwin and M. E. G. Lyons, *Electrochem. commun.*, 2013, DOI:10.1016/j.elecom.2013.03.040.
6. H. Bode, K. Dehmelt and J. Witte, *Electrochim. Acta*, 1966, DOI:10.1016/0013-4686(66)80045-2.
7. R. L. Doyle and M. E. G. Lyons, in *Photoelectrochemical Solar Fuel Production: From Basic Principles to Advanced Devices*, 2016.
8. R. L. Doyle, I. J. Godwin, M. P. Brandon and M. E. G. Lyons, *Phys. Chem. Chem. Phys.*, 2013, DOI:10.1039/c3cp51213d.

9. M. E. G. Lyons and M. P. Brandon, *J. Electroanal. Chem.*, 2010,

DOI:10.1016/j.jelechem.2009.11.024.

10. J. Kibsgaard and I. Chorkendorff, *Nat. Energy*, 2019, DOI:10.1038/s41560-019-0407-1.